Microstructural characterisation of tungsten coatings deposited using plasma sputtering on Si substrates

E. Vassallo [a,*], R. Caniello [a], M. Canetti [b], D. Dellasega [a,c], M. Passoni [a,c]

[a] Istituto di Fisica del Plasma, CNR, via R. Cozzi 53, 20125 Milano, Italy
[b] Istituto per lo Studio delle Macromolecole, CNR, via Bassini 15, 20133 Milano, Italy
[c] Dipartimento di Energia, NEMAS, Politecnico di Milano, via Ponzio 34/3, 20133 Milano, Italy

Article history:
Received 4 September 2013
Received in revised form 13 March 2014
Accepted 14 March 2014
Available online 21 March 2014

1. Introduction

Transition metal films are interesting materials in view of the possibility of growing functional coatings with tailored properties [1,2]. Among these, tungsten (W) and W-based alloyed thin films possess many attractive properties, such as high melting temperature, high mechanical strength, and good metal barrier performance, and thus have potential applications in X-ray field as absorbing layers [3] and mirrors [4] and in semiconductor interconnect layers as diffusion barriers [5–7]. Unfortunately, the thin film stress often determines the limit of film thickness without cracking, buckling, or delamination [8] with difficulties for their technical applications. It is well known that thin films develop large intrinsic stress during the deposition process. The intrinsic stress either originates from strained regions within the films (grain boundaries, dislocations, voids, impurities, etc.) or at the film/substrate (lattice mismatch, different thermal expansion, etc.) interface. Several methods such as rf-substrate biasing [9] and substrate temperature [10] techniques have been proposed to reduce the intrinsic stress of coatings. In the present work, we present the structural and morphological properties evaluated by atomic force microscopy, X-ray diffraction and scanning electron microscopy–energy dispersive spectrometry of W thin films deposited by an RF Plasma system in diode configuration [11] with microstructure in multilayer as a function of the pressure and sputter gas.

* Corresponding author. Tel.: +39 2 66173245; fax: +39 2 66173239.
E-mail address: vassallo@ifp.cnr.it (E. Vassallo).

2. Experimental details

An RF plasma system [12] has been used to produce W coatings. Coatings with thickness in the range of 1 μm were grown on Si substrates (1×1 cm^2, thickness = 400 μm). The experimental apparatus consists of a parallel-plate, capacitive-coupled system, made up of a cylindrical stainless steel vacuum chamber with an asymmetric electrode configuration. A powered electrode is connected to an RF (13.56 MHz) power supply, coupled with an automatic impedance matching unit, while the other electrode, made up of stainless steel, is grounded. A 3-in diameter target of W (purity 99.9%) was placed on the powered electrode. Si substrates were placed on the ground electrode at 6.5 cm away from the powered electrode. No bias voltage and heating were applied to the substrate holder. The substrate temperature was monitored by a thermocouple fixed directly on the substrate. Before the process, the substrates were cleaned with chemical etching solutions to remove surface contaminants. The process chamber was pumped to a base pressure below 1×10^{-5} Pa; high-purity gases were introduced into the vacuum chamber through a mass flow controller in order to establish the desired working pressure. Ar or Ne was used as sputter gas. The RF power was fixed at 150 W (1500 V of DC self-bias voltage). The target was water cooled, and the temperature was kept below 20 °C during the coating process.

The morphological properties and physical structure of the films were investigated by scanning electron microscopy (SEM). Measurements were performed using a ZEISS Supra System with an accelerating voltage of 5 kV. Elemental analysis (EDS) was performed using an INCA detector from Oxford Instruments using 15 kV as accelerating voltage.

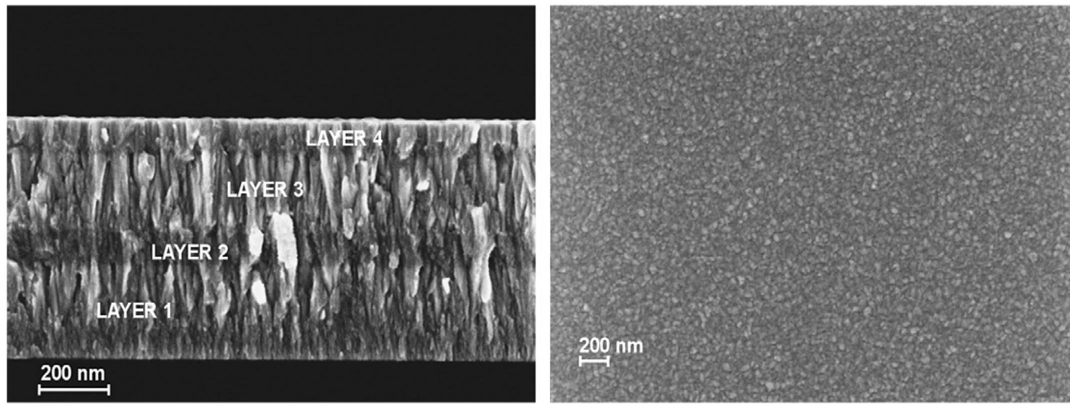

Fig. 1. (left) Cross-sectional and (right) top view SEM images of a multilayer W film produced with Ne as sputter gas.

The structural properties studied by X-ray diffraction measurements were performed with a wide angle Siemens D-500 diffractometer (WAXD) equipped with a Siemens FK 60-10 2000W tube. The radiation was a monochromatized Cu Kα beam with wavelength $\lambda = 0.154$ nm. The operating voltage and current were 40 kV and 40 mA, respectively. The data were collected from 20 to 80 2θ° at 0.02 2θ° intervals by means of a silicon multi-cathode detector Vortex-EX (SII). The roughness was investigated by atomic force microscopy (AFM). Measurements were made in air by a Nano-RTM System (Pacific Nanotechnology, Santa Clara, CA, USA) operating in contact mode. The deposition rates were measured by a P15 surface profiler (KLATencor San Jose, CA) and by SEM.

3. Results and discussion

At first single W layers have been grown at a power of 150 W by setting the pressure between 0.8 and 3 Pa using two types of sputter gas (Ar and Ne). In all these experiments, the films start to delaminate and peel off once thicker than 200–300 nm. The films gradually start to delaminate (in a few minutes) after being taken out of the coating chamber and brought in atmospheric pressure at room temperature. Delamination buckling patterns were observed in such films. The delamination pattern was in the form of random wrinkles. The buckling of the films extended from the outer edge of the substrate towards its interior. This kind of coating instability can be attributed to the development of high residual compressive stress during the deposition process [13]. In all experiments, the maximum measured temperature of the substrates during the deposition process was in the range 50–80 °C, at this temperature the “thermally induced” stress value can be assumed negligible. Therefore in our samples the stress values are mostly incorporated during the film growth. Because all the deposited single layer coatings have shown stress phenomena, in order to relieve the stress, a strategy of deposition in multilayer coating has been used. As we know, the intrinsic stress in sputtered films is correlated to Thornton's structure zone model (SZM) [14,15], which relates the microstructures of sputtered films to the most prominent deposition parameters (for example, the working-gas pressure). An approach by Windt [16] demonstrated that the net stress in a bilayer metal film is minimized by balancing the stresses in the two metal layers, and a clear dependence on gas pressure was stated. In our approach, multilayer coating has been grown in the same plasma conditions and compared with single coating. All coatings produced with microstructure in multilayer showed no stress phenomena. Multilayered W coatings were realized by using the strategy of alternating high and low gas pressures (2 and 0.8 Pa). After the first deposition step (first layer) at high pressures, the working gas process was decreased in-situ, then the deposition was run again. The process was repeated to form thick multilayer films. The reduced ion bombardment at high pressures (enhanced collision and scattering) slows down the adatom mobility and therefore results in less dense films. In this case, the columns are separated from each other by voids that are lower density regions. We can expect that the coating will relieve the stress in the interface between the layers and through the less dense layers. This results in larger critical thickness and better quality films. Likewise, adhesion of films was improved. The adhesion property of the coatings to the Si substrate was tested in accordance with standard D3330 (Method for Peel Adhesion of Pressure-Sensitive Tape of 180° Angle) of the American Society for Testing Materials (ASTM) [17]. All multilayer coatings have passed the scotch tape peel test exhibiting a good adhesion. Fig. 1 shows respectively SEM cross-section and top view micrographs of a multilayer W coating grown by the sequential deposition of four layers alternating high and low Ne gas pressures. The deposition rate of layers grown at high

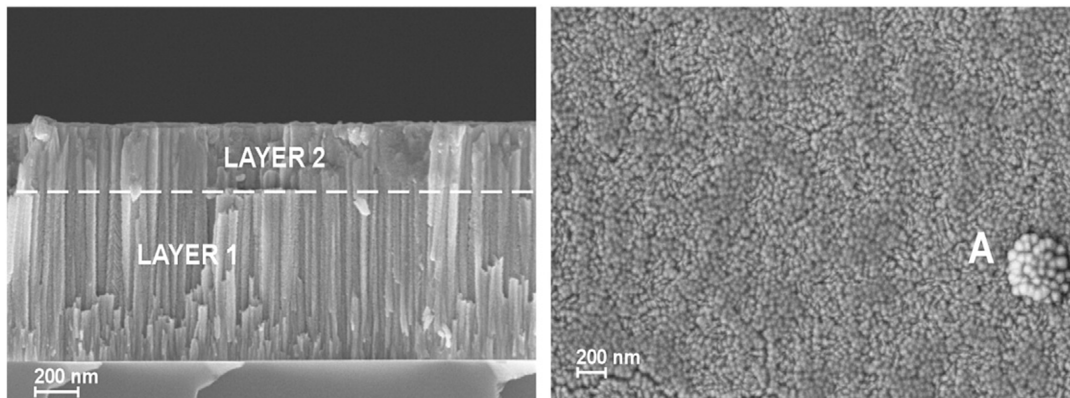

Fig. 2. (left) Cross-sectional and (right) top view SEM images of a multilayer W film produced with Ar as sputter gas.

pressures was 3.6 nm/min, while at low pressure was 1.5 nm/min (total coating thickness ≅ 600 nm). A typical columnar feature of the grains is evident (Fig. 1, left), furthermore, the interface between the W thin film and the substrate is sharp and flat with a good interlayer contact. It can be seen from Fig. 1 (right) that the surface particles of the W films are very fine and uniform, and the average grain size is in the range of 20–30 nm. The sample displayed a smooth surface in which the roughness value (R_{rms}), measured with the fixed area of $2 \times 2\ \mu m^2$, was 4.3 nm.

Fig. 2 (left) shows SEM micrographs of a multilayer W coating grown in the same experimental conditions by the sequential deposition of two layers alternating high and low Ar gas pressures. The deposition rate of layers grown at high pressures was 13.1 nm/min, while at low pressure was 3.2 nm/min (total coating thickness ≅ 1000 nm). Also in this experiment, the coating shows a columnar structure with similar feature of the previous case, however, the surface morphology differs. The grain size is similar, but the coating shows a less dense structure than the Ne case. In addition, the coating shows many cauliflower-like agglomerations in the surface (marker A), and the surface RMS roughness value was found to be 8.5 nm. The deposition rate (Fig. 3) of W was determined as a function of RF power, as expected, it increases with increased mass of sputtering ions due to momentum exchange.

Depending on the growth conditions, W thin films are usually made up of either the stable α phase (bcc lattice), the metastable β phase (A15 cubic lattice), or a mixture of both phases [6]. Fig. 4 (top) shows the XRD patterns of the deposited W films prepared by Ar as sputter gas. The films are composed of a mixture of both phases. In 2θ range from 34° to 42°, we observed the strongest (110) reflection of α-W and (200) reflection of β-W.

The XRD pattern for W films prepared by Ne, in the same plasma conditions, is illustrated in Fig. 4 (down). A significant effect that Ne gas has on the formation of α-W phase is evident. In this case, there are no diffraction peaks of β-W in the overall diffraction range. A new (200) and (112) reflection of α-W at around 58.2° and 73.1°, respectively was observed. On the other hand, a loss of crystallinity can be assessed, indeed, peak broadening and intensity were detected.

As reported in the literature, the formation of β-W phase has shown to be sensitive to a variety of film preparation parameters. Dooho Choi et al. [18] reported that a high base pressure prior to the film deposition produces β-W phase rich coatings. This effect is directly related to the amount of impurities in the chamber. In particular, the correlation of the oxygen contamination and formation of the β phase has been observed repeatedly [19]. In order to reduce the oxygen contamination, a H_2 plasma pre-treatment of the Si substrate was performed for 30 min. W coating was subsequently grown in the same plasma conditions used with Ar as sputter gas (Fig. 4, top). A similar deposition rate (~8 nm/min) was obtained in both depositions. As can be seen in Fig. 5, the W coating showed a microstructure mainly composed

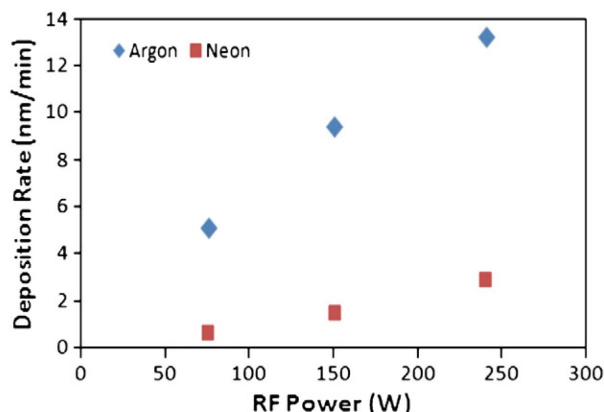

Fig. 3. Deposition rate of W as a function of RF power varying the sputter gas.

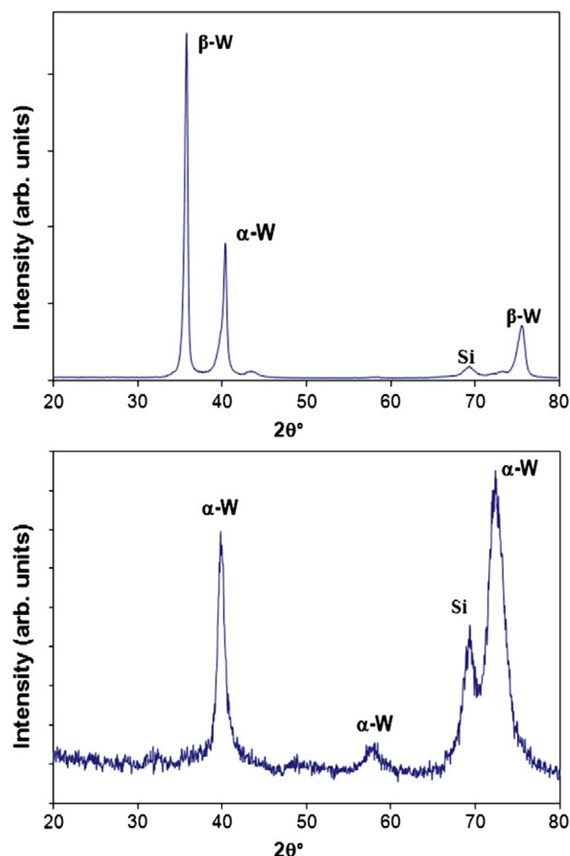

Fig. 4. XRD patterns of multilayer W films: (top) produced with Ar as sputter gas (down) produced with Ne.

of β phase. This result can be attributed to the hydrogen radicals in prolonged Si surface treatment. Johnson et al. [20] and Jeng et al. [21] suggested that defects could be created by hydrogenation. In the early stage of the hydrogen plasma treatment, the hydrogen radicals remove surface contaminants, weak Si – Si bonds and break native Si – O bonds at the top surface to create voids and dangling bonds. Water contact angle measurements confirm the increase of surface energy of Si substrate. The contact angle (Fig. 6) of Si substrate was 70° without H_2 pre-treatment and it decreased with increasing of the pre-treatment time. However, hydrogen diffuses into the silicon sub-surface after a prolonged surface treatment and breaks Si – Si bonds, thus creating new defects that increase for a

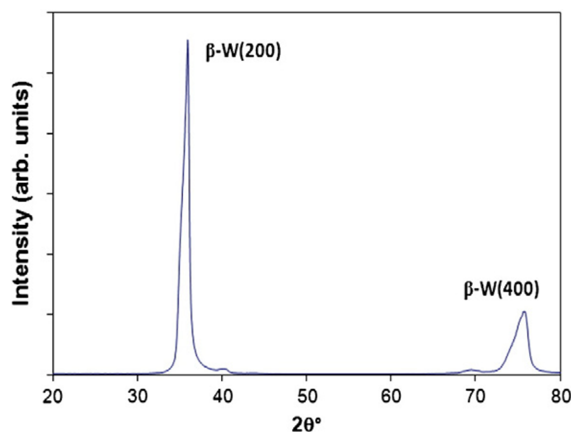

Fig. 5. XRD patterns of multilayer W films produced with Ar as sputter gas and with 30 min of H_2 plasma pre-treatment.

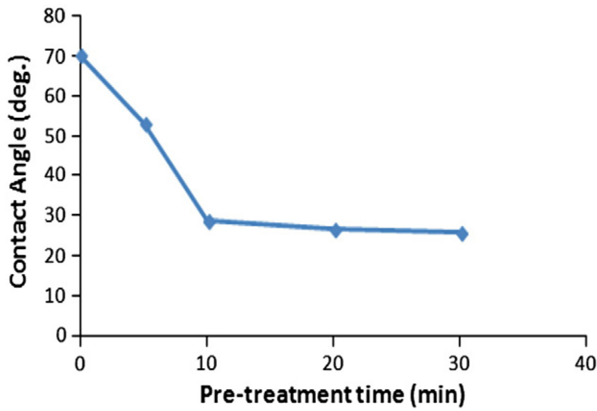

Fig. 6. Contact angle as a function of H2 plasma pre-treatment time for Si substrate.

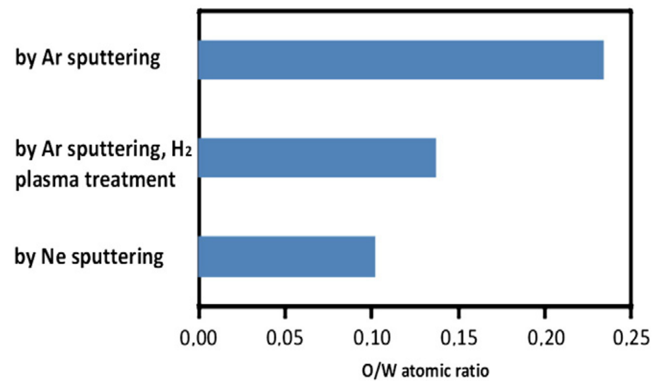

Fig. 8. O/W ratio evaluated by EDS. Samples (1) Ar as sputter gas, (2) Ar as sputter gas and H_2 plasma pre-treatment, (3) Ne as sputter gas.

longer process time. In order to analyze the effect of the crystalline orientation of the substrate on the growth direction of the coatings, different W coatings were grown in the same plasma conditions on Si with different orientations (Si(100) and Si(001)). As expected, for each substrate type, the growth of the W is predominantly oriented, yielding the same peaks. This is due to the large mismatches between W and the growth substrate used. Fig. 7 shows respectively SEM top view and cross-section micrographs of a multilayer W coating grown in the same experimental conditions used with Ar sputter gas, but with a H_2 plasma pre-treatment of the Si substrate performed for 30 min. The coating shows a columnar structure with similar feature of the Ar case. The surface morphology is similar, however, in this case there are very few cauliflower-like agglomerations in the surface (marker B), and the surface RMS roughness is 9.3 nm. The composition of coatings grown in the same experimental conditions was evaluated by EDS. The deposited coatings were composed of W and O atoms. Fig. 8 shows the O/W atomic ratio of coatings produced by using Ar sputtering, Ar sputtering with H2 plasma pre-treatment and Ne sputtering. The presence of oxygen in the coatings can be due to the residual oxygen and water vapor in the deposition chamber and to the exposure of coatings in ambient atmosphere before the EDS analysis. Since the base pressure before all the depositions is the same, we attribute the higher amount of oxygen in the coatings mainly to the exposure in ambient atmosphere. As demonstrated by SEM investigations, the coating (sample 3) grown by Ne as sputter gas is more dense than the other samples, this explains the lower value of O/W ratio. Regarding samples 1 and 2, another consideration is that even though sample 2 shows similar features of sample 1 (Figs. 2 and 7), a marked decrease of the oxygen is evident. We can speculate that the H_2 plasma pre-treatment contributes to the reduction of oxygen contamination before deposition, furthermore, the increase of the surface energy (Fig. 6) has driven the growth of a denser coating (this last statement needs to be confirmed by nuclear reaction analysis). Another interesting result from EDS analysis is the concentration of inert gas embedded in deposited tungsten. For all coatings deposited by Ar as sputter gas, no concentration of inert gas was found (below the detection limit of our spectrograph). In the case of Ne, embedded gas was found (in the range 10–12%) in all coatings.

4. Conclusions

Nanostructured W coatings have been deposited by an RF plasma system in diode configuration. The intrinsic stress of coatings has been eliminated using a microstructure in multilayer formed by passing from high to lower working-gas pressure. This stress control strategy has provided stress reduction and a high critical thickness for deposited W thin films. These multilayer thin films have exhibited good adhesions to the substrates thereby avoiding delamination. The results showed that the coating crystalline structure can be tuned by varying the process gas. The analyses illustrate the shift from a mixture of both α and β phases to a dominated structure by α phases for Ne discharges. The coating grown with Ne is denser with smaller grain size, and thus has a smoother surface. On the other hand, a loss of crystallinity has been detected. The structure can be also tuned by a H_2 plasma pre-treatment of the substrate, the W coating showed a microstructure composed of β phase. All coatings showed a morphology with flat surface and low roughness.

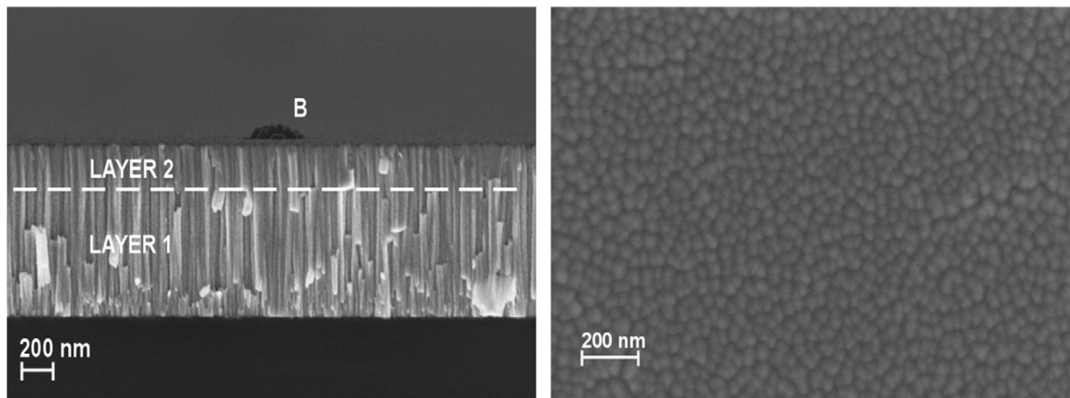

Fig. 7. (left) Cross-sectional and (right) top view SEM images of a multilayer W film produced with Ar as sputter gas and H_2 plasma pre-treatment of the Si substrate.

References

[1] P.R. Bueno, F.M. Pontes, E.R. Leite, L.O.S. Bulhoes, P.S. Pizani, P.N. Lisboa-Filho, W.H. Schreiner, Structural analysis of pure and $LiCF_3SO_3$-doped amorphous WO_3 electrochromic films and discussion on coloration kinetics, J. Appl. Phys. 96 (2004) 2102.

[2] L. Meda, R.C. Breitkopf, T.E. Haas, R.U. Kirss, Investigation of electrochromic properties of nanocrystalline tungsten oxide thin film, Thin Solid Films 402 (2002) 126.

[3] M. Itoh, M. Hori, S. Nadahara, The origin of stress in sputter-deposited tungsten films for x-ray masks, J. Vac. Sci. Technol. B 9 (1991) 149.

[4] A.T.T. Mostako, C.V.S. Rao, Alika Khare, Mirrorlike pulsed laser deposited tungsten thin film, Rev. Sci. Instrum. 82 (2011) 013101.

[5] K.Y. Ahn, A comparison of tungsten film deposition techniques for very large scale integration technology, Thin Solid Films 153 (1987) 469.

[6] S.M. Rossnagel, I.C. Noyan, J.C. Cabral, Phase transformation of thin sputter-deposited tungsten films at room temperature, J. Vac. Sci. Technol. B 20 (2002) 2047.

[7] V.G. Glebovsky, V.Y. Yaschak, V.V. Baranov, E.L. Sackovich, Properties of titanium-tungsten thin films obtained by magnetron sputtering of composite cast targets, Thin Solid Films 257 (1995) 1.

[8] K.D. Lee, E.T. Ogawa, S. Yoon, X. Lu, P.S. Ho, Electromigration reliability of dual-damascene Cu/porous methylsilsesquioxane low *k* interconnects, Appl. Phys. Lett. 82 (2003) 2032.

[9] A. Bensaoula, J.C. Wolfe, A. Ignatiev, F.O. Fong, T.S. Leung, Direct-current-magnetron deposition of molybdenum and tungsten with rf-substrate bias, J. Vac. Sci. Technol. A 2 (1984) 389.

[10] R. Rastogi, V. Dharmadhikari, A. Diebold, Stress variation with temperature/time and its correlation to film structure and deposition parameters, J. Vac. Sci. Technol. A 9 (1991) 2453.

[11] R.F. Bunshah, Handbook of Deposition Technologies for Films and Coatings, Noyes Publications, U.S.A., 1994. 50.

[12] H.R. Koenig, L.I. Maissel, IBM J. Res. Dev. 14 (1970) 168.

[13] D.C. Meyer, A. Klingner, T. Holz, P. Paufler, Self-organized structuring of W/C multi-layers on Si substrate, Appl. Phys. A Mater. Sci. Process. 69 (1999) 657.

[14] J.A. Thornton, Thorton's structure zone diagram for sputtering, J. Vac. Sci. Technol. 11 (1974) 666.

[15] J.A. Thornton, High rate thick film growth, Annu. Rev. Mater. Sci. 7 (1977) 239.

[16] David L. Windt, Low-stress W/Cr films for SCALPEL® mask scattering layers, J. Vac. Sci. Technol. B 17 (1999) 1385.

[17] W.J. Chou, G.P. Yu, J.H. Huang, Mechanical properties of TiN thin film coatings on 304 stainless steel substrates, Surf. Coat. Technol. 149 (2002) 7.

[18] Dooho Choi, Bincheng Wang, Suk Chung, Xuan Liu, Amith Darbal, Adam Wise, Noel T. Nuhfer, Katayun Barmak, Phase, grain structure, stress, and resistivity of sputter-deposited tungsten films, J. Vac. Sci. Technol. A 29 (2011) 051512.

[19] J. Ligot, S. Benayoun, J.J. Hantzpergue, Characterization and modeling of electrical resistivity of sputtered tungsten films, J. Vac. Sci. Technol. A 19 (2001) 798.

[20] N.M. Johnson, F.A. Ponce, R.A. Street, R.J. Nemanich, Defects in single-crystal silicon induced by hydrogenation, Phys. Rev. B 35 (1987) 4166.

[21] S.J. Jeng, G.S. Oehrlein, G.J. Scilla, Hydrogen plasma induced defects in silicon, Appl. Phys. Lett. 53 (1988) 1735